Minami Kataoka,[1] Sang-Sun Jeong,[2] Yuzo Obara,[2] Toru Yoshinaga,[2] Yoji Mine,[3] and Kazuki Takashima[3]

Testing Method for Determination of Microscopic Fracture Toughness for Rock Materials

Reference

[1] Department of Systems Innovation, University of Tokyo, 7-3-1 Hongo Bunkyo-ku, Tokyo 113-8656, Japan (Corresponding author), e-mail: mkataoka@sys.t.u-tokyo.ac.jp, https://orcid.org/0000-0002-3325-9655

[2] Department of Civil and Environmental Engineering, Kumamoto University, 2-39-1 Kurokami Chuo-ku, Kumamoto 860-8555, Japan

[3] Department of Materials Science and Engineering, Kumamoto University, 2-39-1 Kurokami Chuo-ku, Kumamoto 860-8555, Japan

ABSTRACT

The fracture behavior of rocks is known to depend on the microstructures of the rocks: the distribution and orientation of the microcracks, and the type, size, and shape of mineral grains. To explain quantitatively the effect of the microstructures on the fracture of rocks, the determination of the fracture toughness of grain and grain boundaries, namely, the microscopic fracture toughness (MFT), is necessary. The authors developed a testing method for determination of MFT for rock materials. A microsized specimen of a cantilever beam type with dimensions of 10 by 10 by 50 µm was used in this testing method, and we built a special testing machine for this specimen. Microsized specimens were made within grains of Iksan granite by Focused Ion Beam machining, and the MFT of its constituents—plagioclase, alkali feldspar, and quartz—was determined using this testing method at room temperature. The MFT varied widely and the results are discussed based on the mineralogical knowledge. This testing method will be helpful to more accurately interpret the fracture behavior.

Keywords

Introduction

The utilization of underground resources has become diversified, enlarged, and complex, e.g., exploitation of energy resources (geothermal energy and shale gas, etc.), underground petroleum storage, carbon dioxide geological storage, and disposal of high-level nuclear waste. The excavation and drilling techniques that are used under higher temperature and pressure for construction of larger and deeper underground spaces, and empirical as well as theoretical estimation methodologies for estimation of the long-term stability of rock structures, must be developed and improved. Mechanisms of rock fracture and especially the linear elastic fracture mechanics (LEFM) have been used to explain rock engineering problems. In LEFM, a mechanical property known as the fracture toughness describing resistance to crack initiation is important for understanding of the fracture behavior of the materials.

Several testing methods have been suggested by the International Society for Rock Mechanics (ISRM) for determining the Mode I (opening mode) fracture toughness of rock materials: the short rod test, chevron bend test, cracked chevron notched Brazilian disk test, and semicircular bend (SCB) test (Franklin et al. 1988; Fowell 1995; Kuruppu et al. 2014). The fracture toughness determined by the testing methods is known to depend on the microstructures of rocks; the distribution and orientation of microcracks; and the type, size, and shape of mineral grains (Nasseri and Mohanty 2008; Kataoka, Obara, and Kuruppu 2011,2015). Rock is an inhomogeneous material. Crystalline rock, such as granite, for instance, consists of a completely crystalline assemblage of minerals and microcracks as mechanical weaknesses are included within mineral grains. Kataoka, Obara, and Kuruppu (2011,2015) estimated the anisotropy of the Mode I fracture toughness of a crystalline rock (Rustenburg granodiorite) by the SCB tests and analyzed the fracture states using X-ray computed tomography images of the specimens after the test. It was reported that the observed fractures tended to go across grains with lower density and along grain boundaries, rather than across grains with higher density, and that the anisotropic characteristics of the fracture toughness were shown because of the orientation of mineral grains. It can be considered that the fracture toughness varied depending on the mineral type of grains and grain boundaries.

The fracture toughness of grains, including their boundaries, which is described as microscopic fracture toughness (MFT) in this article, is an important property in understanding the fracture behavior of rock materials. To estimate the microscopic mechanical properties (the elastic modulus, tensile strength, fracture toughness, and fatigue life) of the alloys used for Micro Electro Mechanical Systems or Micro System Technology devices, a mechanical testing machine for a microsized specimen was developed by Higo et al. (2000). Takashima and Higo (2005) and Halford et al. (2005) estimated the fracture toughness of amorphous and fully lamellar alloys using the microsized specimens and investigated the effects of the specimen size on fatigue and fracture. If this testing method can be introduced to the field of rock mechanics, it should be useful and effective in evaluating the MFT to explain quantitatively the effect of the microstructures on the fracture behavior and to clarify the fracture mechanisms of rocks.

Recently, the authors proposed a testing method for determination of MFT for rock materials (Kataoka et al. 2014; Jeong, Obara, and Kataoka 2016; Jeong et al. 2017). However, only a few experiments were performed during the investigations, and the discussion of the size effect on the fracture toughness and the variation of the MFT given was not sufficient. In this article, this new testing method is introduced to measure the MFT of granite, and the test results (including new ones) are reported. Microsized specimens were prepared using Iksan granite with Focused Ion Beam (FIB) machining to be tested using the special testing machine developed for this purpose. The MFT of plagioclase, alkali feldspar, and quartz within the granite was determined using this testing method at room temperature. The determined MFT was discussed based on the mineralogical knowledge. The size effect on the fracture toughness and the variation of the MFT were also investigated.

Testing Method

DETERMINATION OF FRACTURE TOUGHNESS

A microsized specimen used for the fracture toughness test is a cantilever beam type with an artificial notch as a crack and is shown in Fig. 1. The dimensions of the beam are approximately 10 µm thick and wide and 50 µm in length. The artificial notch with a depth of approximately 3 µm is located near the fixed end of the cantilever beam. Load is applied at a point on the side surface at a distance of 30 µm from the notch by a diamond chip with a curvature of 5 µm. The Mode I fracture toughness, K_{IC}, as a critical value of the stress intensity factor, is estimated from maximum load P_{max} using the following equation for the stress intensity factor for a single edge notched cantilever beam (Murakami 1987):

$$K_{IC} = \frac{6P_{max}S}{W^2 B} \sqrt{\pi a} Y(a/W) \qquad (1)$$

where:

a = depth of the artificial notch,
W = thickness of the cantilever beam,
B = width of the cantilever beam,

FIG. 1 SIM image of a microsized specimen, which is made using quartz (No. Q-3 in **Table 2**) from Iksan granite (after Jeong, Obara, and Kataoka 2016).
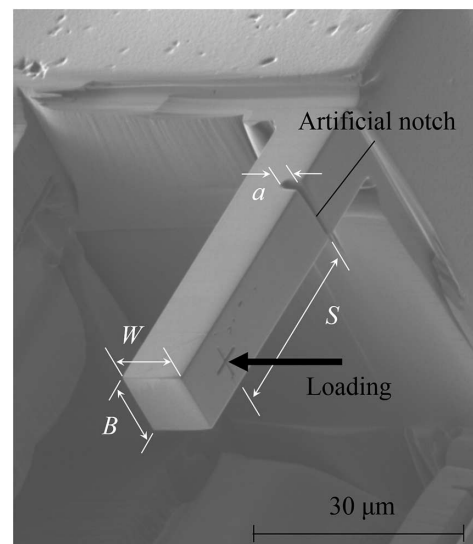
$S =$ distance between the loading point and the notch, and
$Y =$ function of dimensionless notch length a/W, as follows:

$$Y(a/W) = 1.122 - 1.40(a/W) + 7.33(a/W)^2 - 13.08(a/W)^3$$
$$+ 14.0(a/W)^4 \qquad (2)$$

SPECIMEN

Iksan granite was used as the test material. This rock was pro-
duced in Iksan, North-Jeolla Province (Jeollabuk-do), Korea.
The uniaxial compression test and Brazilian disk tensile test of
this rock were performed using a few centimeters of specimens
(Kataoka, Obara, and Kuruppu 2015). The elastic wave velocity
of this rock was also measured (Kataoka and Obara 2013;
Kataoka, Obara, and Kuruppu 2015), and the results are listed
in **Table 1**. A thin section was observed using a polarization micro-
scope to investigate the composite minerals and the microstruc-
tures. The mineral types of quartz, plagioclase, alkali feldspar,
biotite, etc. were found, as shown in **Fig. 2**, and the average grain
size was estimated as 0.6–0.8 mm (Kataoka and Obara 2013;
Kataoka, Obara, and Kuruppu 2015).

To prepare the microsized specimen, a rock block was cut
into a rectangular parallelepiped with dimensions of 3 by 5 by
7 mm, as shown in **Fig. 3a**. The surfaces of the rectangular par-
allelepiped were polished smoothly and the microsized specimen
was prepared along a side that was 7 mm in length. To determine
the MFT of a single mineral grain, the microsized specimen was
prepared within grain-avoiding flaws (such as microcracks). An
Electron Probe Microanalyzer (EPMA) was used to specify the
mineral types of a grain.

Microsized specimens were made by a FIB instrument
(Quanta 3D 200i, Fei Company, Hillsboro, OR). Prior to the start
of the preparation, the surfaces of the rectangular parallelepiped
were coated with gold by sputter deposition. The rectangular par-
allelepiped was then fixed into a holder to allow FIB microma-
chining. The FIB instrument uses a gallium ion source and
operates at an accelerating voltage of 30 kV with a walking dis-
tance of 30 mm. **Fig. 3b–d** shows the preparation process of the
microsized specimen. FIB hits gray areas on the rectangular par-
allelepiped surfaces shown in **Fig. 3b** and **c** at a current of 20 or
7 nA. The materials in these areas are removed by micromachin-
ing with FIB sputtering. The shape of a cantilever beam was made

TABLE 1 Material properties of Iksan granite (after Kataoka et al.
2013,2015).

Properties	Values
Uniaxial compressive strength	167–170 MPa
Young's modulus	19.0–19.2 GPa
Tensile strength	10.3–11.4 MPa
Elastic wave velocity	4.0–4.2 km/s

FIG. 2 Mineral grains of Iksan granite as shown in a thin section. The
scale of the microsized specimen is indicated (Kataoka et al.
2014; Jeong et al. 2016,2017).
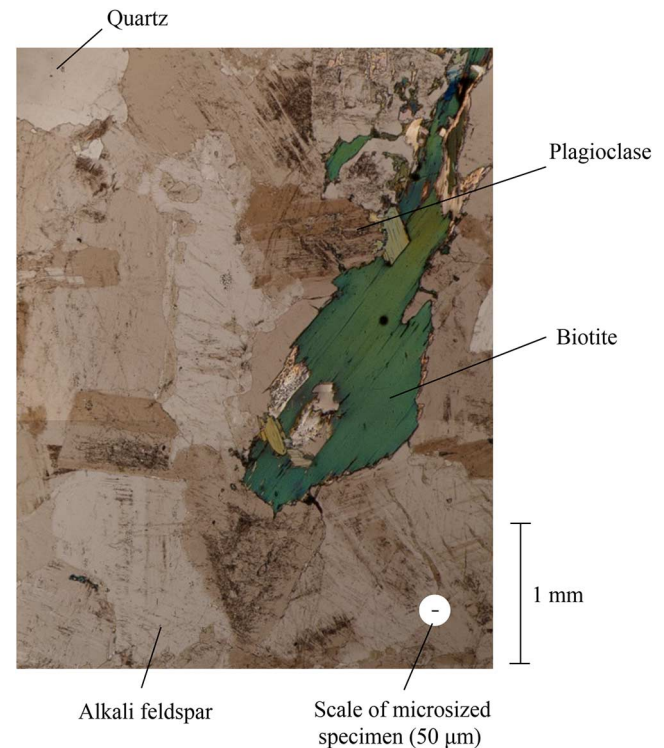
roughly at such a high current. After this process, the surfaces of
the cantilever beam were made smooth by FIB using a lower
current of 3 nA, making the beam size, as shown in **Fig. 1**. The
dimensions of the beam were measured by a Scanning Ion
Microscope (SIM) with an image resolution of 0.1 μm. Then,
the artificial notch and the alignment markings of the loading
point were prepared by FIB machining. To make the depth of
the artificial notch approximately 3 μm, a thin FIB at a current
of 0.1 nA was emitted in the direction of the beam width, and the
curvature of its tip was made to 0.25 μm. This preparation process
does not need a special FIB operation skill because of the simple
shape of the specimen. Moreover, the effect of mineral types on
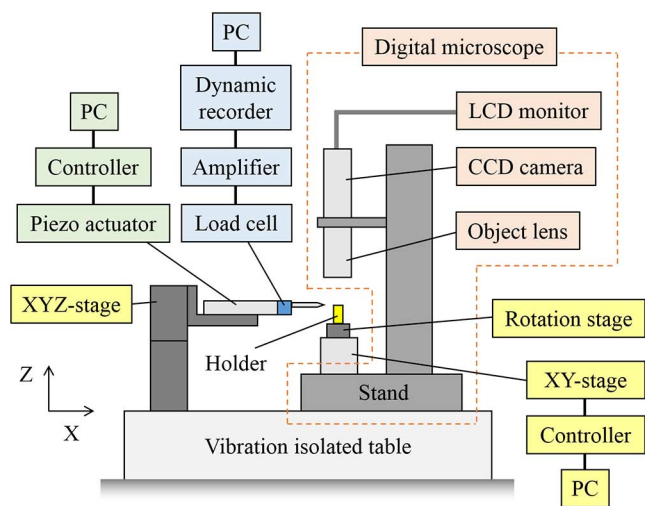the machining speed and accuracy showed little difference.

TESTING MACHINE

The authors built a testing machine for the fracture toughness test
using the microsized specimens. A block diagram of this testing
system and the view of the specimen are shown in **Figs. 4** and **5**,
respectively. The advantage of this testing machine is that a po-
sition alignment and the loading of the microsized specimen are
provided by using six accurate stages, a piezo actuator, and a high-
powered digital microscope. This testing machine was fixed on a
vibration isolated table. The microsized specimen within the rec-
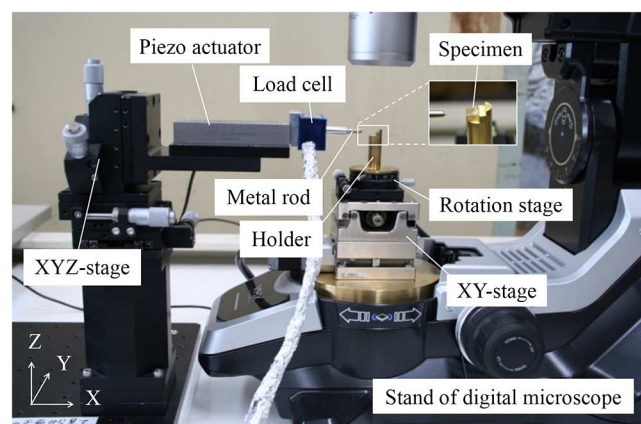tangular parallelepiped is put on a loading holder fixed on a

FIG. 3

Preparation of microsized specimen: (a) rectangular parallelepiped of Iksan granite; (b)–(d) preparation process by FIB (after Kataoka et al. 2014; Jeong, Obara, and Kataoka 2016).
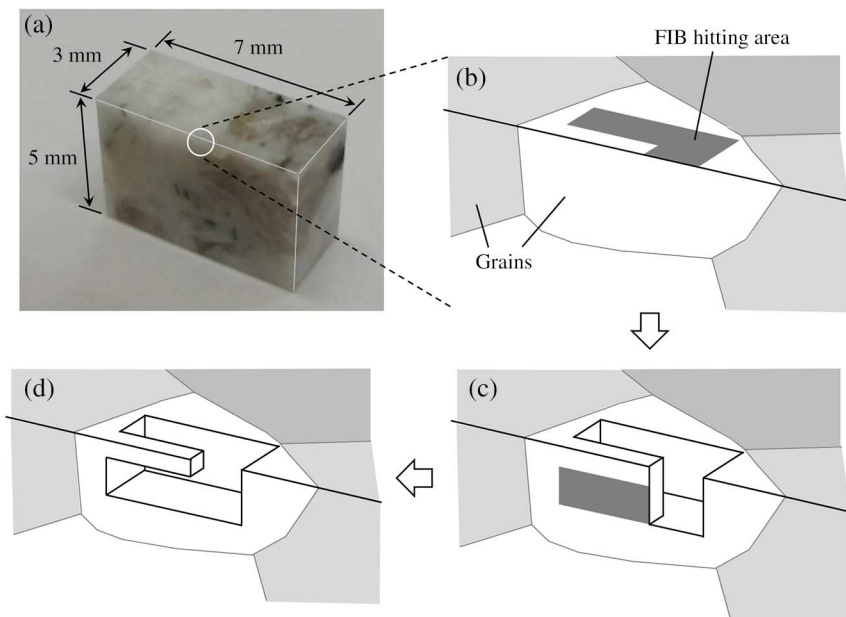
FIG. 4 Block diagram of testing system for the microsized specimen. To provide a position alignment of the microsized specimen for loading, six accurate stages are equipped with a high-powered digital microscope (after Jeong, Obara, and Kataoka 2016).

rotation stage with a rotation resolution of 0.2° and an XY-stage with a translation resolution of 0.1 μm.

A metal rod is attached to an actuator, which is installed on manual type XYZ-stages with a translation resolution of 0.1 μm. A diamond chip with a curvature of 5 μm is installed at the tip of the metal rod. The load is applied by the diamond chip at the loading point of the microsized specimen. The lateral displacement of the metal rod with the diamond chip is applied by a

FIG. 5 View of the specimen placed at the mechanical testing system (after Jeong et al. 2016,2017).

piezoactuator with a resolution of 0.2 nm and a maximum stroke of 38 μm. With the six stages installed in the testing system, the positions of the microsized specimen and the diamond chip, and its loading direction can be adjusted with accuracy.

The rotation stage and XY-stage are fixed on a stand of a VHX-5000 digital microscope (Keyence, Osaka, Japan). The loading state shown in **Fig. 6**, as well as the adjustment of the positions of the specimen, can be observed in real time by the digital microscope with a magnification of 250 to 2,500. Load is measured by a load cell with a resolution of 20 μN and a maximum of 200 mN equipped to the actuator. The loading rate was 0.1 μm/s, and the sampling interval was 10 μs.

FIG. 6

Loading state observed by the digital microscope with a magnification of 2,500: (a) start of the loading, (b) end of the loading. The crack propagation from the artificial notch tip can be observed (after Jeong, Obara, and Kataoka 2016).

(a)   (b)
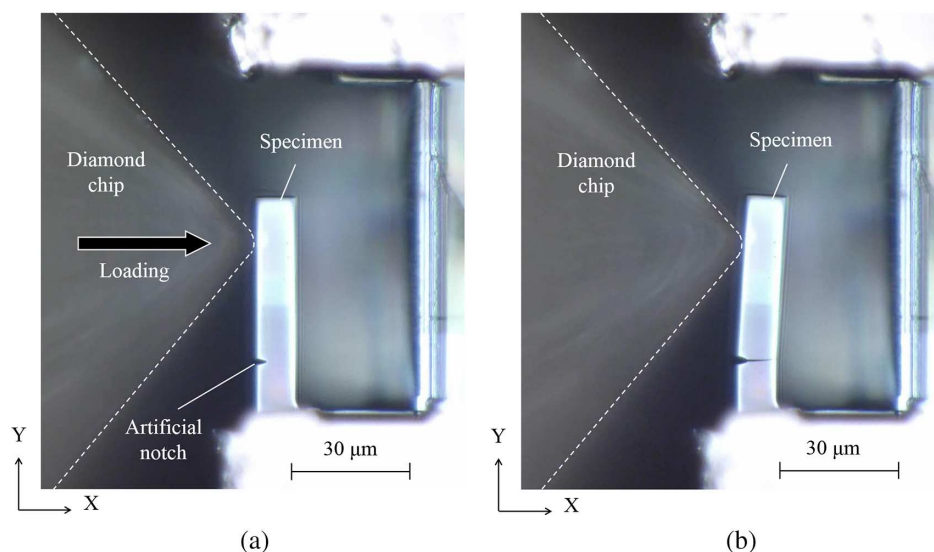
Experimental Results

The fracture toughness test was conducted at room temperature using the developed testing machine. The mineral type and size of microsized specimens and the test results are summarized in **Table 2**. The microsized specimens were prepared within the grains of plagioclase, alkali feldspar, and quartz of Iksan granite.

Load-displacement curves in the fracture toughness test are shown in **Fig. 7**. The load increases linearly with increasing displacement and the fracture suddenly occurs just after reaching maximum load, P_{max}, for all the specimens. Both the P_{max} value and the slope of the curve (deformability) vary widely from one specimen to the other, although in the same mineral type. The value of MFT K_{IC} was determined from the value of P_{max} using Eq 1. The MFT is also highly variable in value.

The fracture surfaces of specimens observed by the SIM after the test are shown in **Fig. 8**. The fractures of the feldspar group (plagioclase and alkali feldspar) shown in **Fig. 8a** and **b** do not initiate and propagate in the direction of the artificial notch straightly. On the other hand, as shown in **Fig. 8c**, the fracture of the quartz propagates straightly in almost the same direction as the artificial notch.

## Discussion

VARIATION OF MFT

The variation of the MFT shown in **Table 2** is dependent on an existence of mechanical weak planes within the microsized specimens. The propagated direction of the fracture changes suddenly

TABLE 2 Specimen dimensions and experimental results.

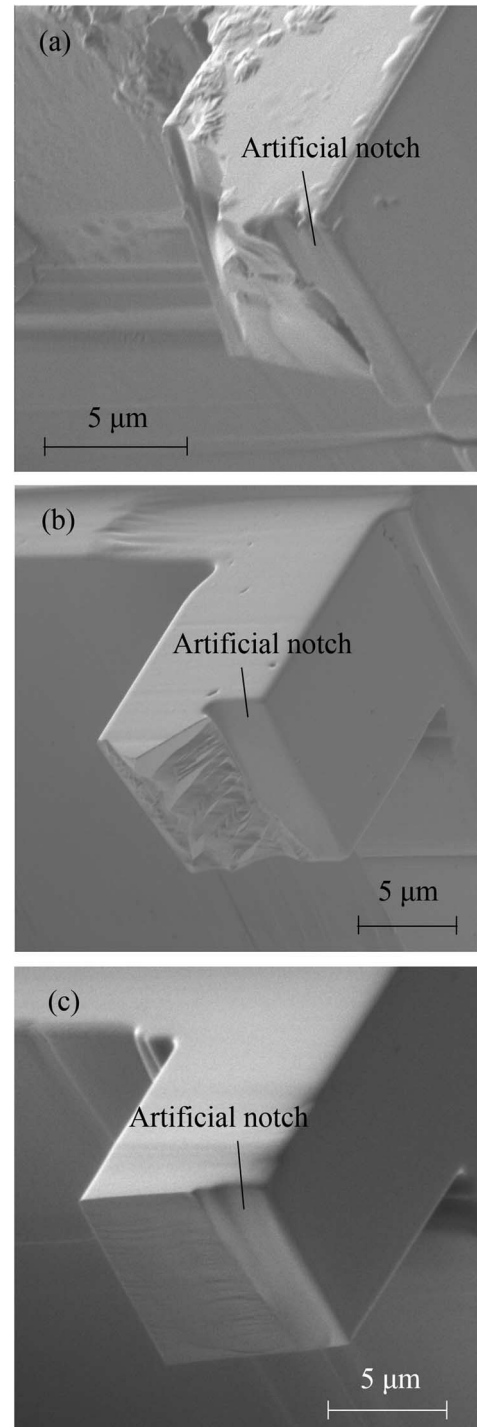| No.	Mineral	W (μm)	B (μm)	S (μm)	a (μm)	P_{max} (mN)	K_{IC} (MN/m$^{3/2}$)
P-1[*]	Pl	10.7	10.4	30.7	3.0	1.22	0.64
P-2	Pl	10.4	10.2	31.4	2.8	1.03	0.57
P-3	Pl	10.2	10.0	30.2	2.2	1.38	0.67
P-4	Pl	10.4	10.2	29.6	2.5	1.05	0.51
A-1[†]	Afs	9.6	11.0	29.4	3.2	0.40	0.25
A-2[†]	Afs	10.6	10.5	29.6	2.5	1.25	0.57
A-3	Afs	10.4	10.4	28.5	2.5	1.18	0.54
Q-1[††]	Qz	10.2	10.9	28.6	2.8	1.68	0.83
Q-2[††]	Qz	10.1	10.0	28.7	3.5	0.82	0.54
Q-3[††]	Qz	9.7	10.2	29.2	2.7	0.23	0.13
Q-4	Qz	10.2	11.2	30.5	2.5	1.75	0.83

Note: Pl = Plagioclase; Afs = Alkali feldspar; Oz = Quartz; W, B, S and a = specimen dimensions shown in **Fig. 1**; P_{max} = maximum load; K_{IC} = Mode I fracture toughness; [*], [†], and [††] at specimen No. heading indicate the data from Kataoka et al. (2014) and Jeong et al. (2016, 2017), respectively.

(a)

(b)

(c)
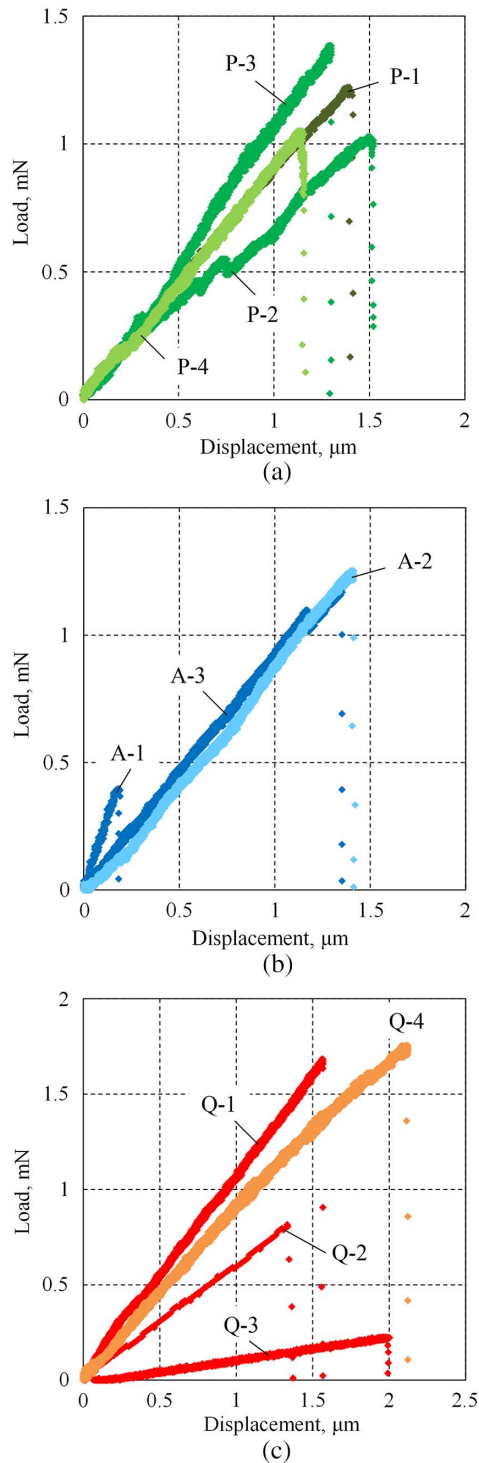
during the fracture process for the feldspar group (**Fig. 8a** and **b**). The feldspar group has two planes of cleavage meeting at or near 90°, forming mechanical weak planes (Lutgens and Tarbuck 1997;

Nave 2017). The fracture state shown in **Fig. 8a** and **b** indicates the existence of cleavage within the specimens of the feldspar group. Moreover, shear fractures appear locally because of the mechanical weak planes in the mineral structure. The fracture may have

been due to the combination of both effects, resulting in the variation of the MFT.

Although the fracture of the quartz group propagates straightly in almost the same direction as the notch (**Fig. 8c**), there is also scattering in the MFT results (**Table 2**). Quartz frequently twins (Association for Geological Collaboration in Japan 1996; Amethyst Galleries, Inc., 1995). Twinning may follow the Dauphine law and the Brazil law and produces prism plane and rhombohedral plane. It is known that breakage occurs easily along these planes (Association for Geological Collaboration in Japan 1996). If the direction of the artificial notch is parallel to these planes, the fracture resistance in this case can be considered lower than that in the other directions. Thus, MFT of quartz is dependent on the direction of fracture. The mechanical weak planes can influence the MFT of rock mineral grains.

SIZE EFFECT ON FRACTURE TOUGHNESS

Jeong et al. (2017) estimated the fracture toughness of Iksan granite using the SCB tests, which is suggested by ISRM as a standard testing method for the Mode I fracture toughness of rock (Kuruppu et al. 2014). In the tests, the semicircular disk specimens with various diameters ranging from 12.5 to 50 mm were used. **Fig. 9** shows the relation between the fracture toughness and the specimen size (the radius r of the SCB specimens). In this figure, the MFT determined in this study is also plotted; the specimen size indicates the thickness W of the cantilever beam. It was observed that the fracture toughness of rocks increased with increasing specimen size. This trend was also observed in previous

FIG. 9 Relation between fracture toughness and specimen size for Iksan granite. The closed and open symbols indicate the values determined by the microsized and SCB specimens, respectively. The broken line indicates the calculated result based on the Bažant size effect law (Bažant 1984).

studies (Ayatollahi and Akbardoost 2014; Kataoka and Obara 2015). The MFT is lower than the fracture toughness determined by the conventionally sized specimens.

As mentioned earlier, the effect of the mechanical weak planes on the MFT is significant in rock. Kataoka and Obara (2015) reported that the crack resistance decreases with the decrease in specimen size because the mechanical weak planes near the notch tip of the specimen can be assumed to be relatively large. The size effect on the fracture toughness of rock from microsized to conventionally sized specimens may be interpreted by this explanation.

Bažant (1984) and Bažant, Gettu, and Kazemi (1991) proposed the size effect low according to the nonlinear fracture mechanics caused by the existence of a microcracking zone, which is called the fracture process zone near the crack tip. The broken line in **Fig. 9** shows the fracture toughness estimated by the SCB specimen calculated based on Bažant (1984), Bažant, Gettu, and Kazemi (1991), and Ayatollahi and Akbardoost (2014). The test results agree with the calculation. K_{IC} for an infinitely large specimen can be calculated as 1.44 MN/m$^{3/2}$ when the specimen radius $r \rightarrow \infty$. However, the MFT tends to be larger than the calculated result for its size. Moreover, the fracture surfaces shown in **Fig. 8** are similar to those of brittle material, such as glass and chalk (Bahat, Rabinovich, and Frid 2001; Gopalakrishnan and Mecholsky 2012). The load-displacement curves (**Fig. 7**) show that the compliance is not changed during increasing load and that the load falls just after reaching its maximum value in a brittle manner. These indicate that the estimation of the MFT is less affected by the fracture process zone. To make the mechanism clearer, a modification considering the nonlinearity (Barker 1979; Matsuki, Hasibuan, and Takahashi 1991) will also be necessary in future work.

MFT can correspond to the microscopic strength considered by Weibull's distribution (Weibull 1951). **Fig. 10** shows the Weibull plot for the fracture toughness K_{IC} of Iksan granite determined by microsized specimens used in this study and the SCB specimens (Jeong et al. 2017). They follow the distribution given in Eq 3:

$$1 - F(K_{IC}) = \exp\left\{-\left(\frac{K_{IC}}{\eta}\right)^m\right\} \quad (3)$$

where:

$F(K_{IC})$ = cumulative distribution function of K_{IC},
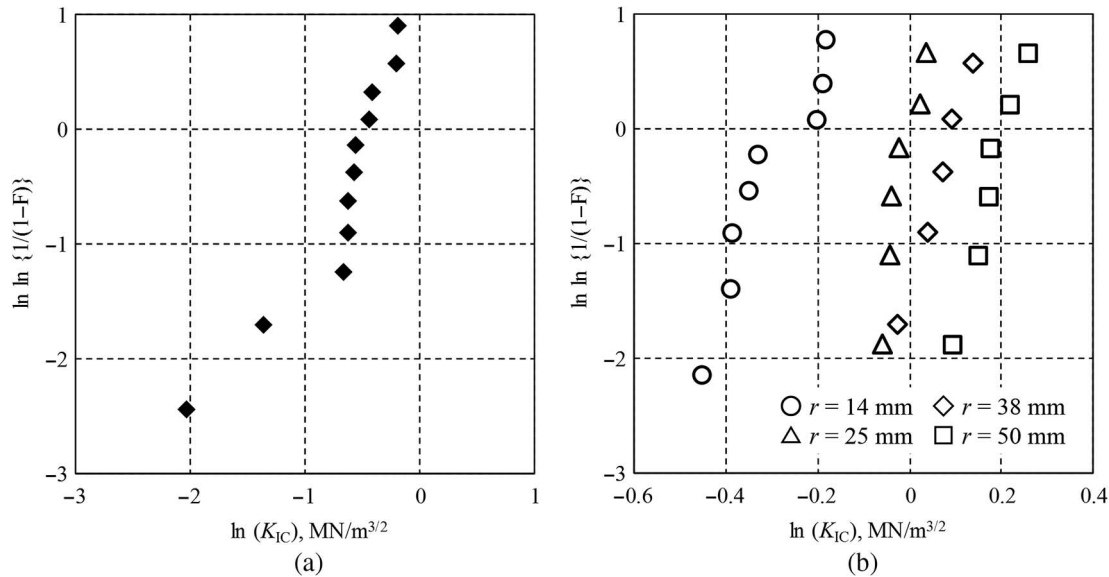
m = shape parameter of the distribution, and

η = scale parameter of the distribution.

m is also known as the coefficient of uniformity, and the value is 1.66 for the MFT. The m value for K_{IC} determined by the SCB specimens with various radii ranged from 8.72 to 21.9 and were higher than that for the MFT. The m values for the uniaxial compressive strength and tensile strength of several rock types tend to be in the range of 10 to 35 (Shin et al. 2005) and are also higher
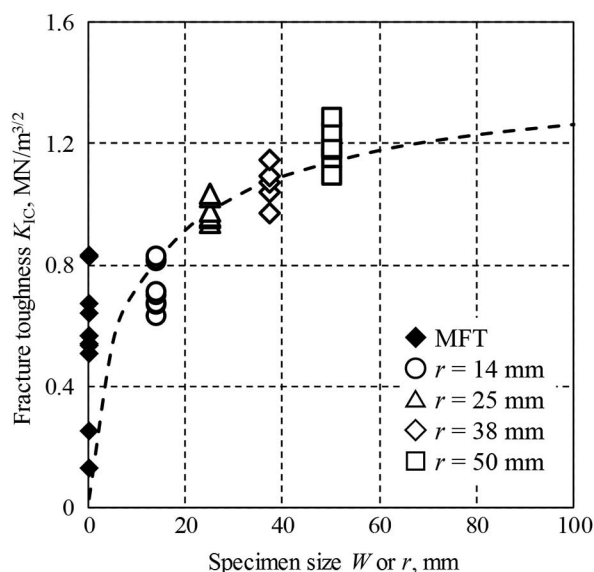
FIG. 10 Weibull plot for the fracture toughness of Iksan granite determined by (a) microsized specimens and (b) SCB specimens. The symbols correspond to the ones in **Fig. 9**.

(a)   (b)

than that for the MFT. The inhomogeneity of rock materials plays a significant role in the fracture behavior of rocks so much so that it has been introduced into the models of some numerical simulations for rock fracturing (Cho, Ogata, and Kaneko 2003). The large variation of the microscopic strength used in previous studies (Tang 1997; Liu et al. 2002) is almost the same as that in the MFT observed in this study. It indicates that the variation of the MFT can be accommodated in the use of numerical simulations of rock fracturing.

Conclusions

A testing method for the determination of the Mode I MFT for rock material was introduced in this article. Microsized specimens were prepared using Iksan granite by FIB machining. A special testing machine for the microsized specimen was developed. The MFT of plagioclase, alkali feldspar, and quartz within the granite was determined using this testing method. Results showed that the MFT varied widely in each microsized specimen, although in the same mineral type. Based on the mineralogical knowledge, it is concluded that the mechanical weak planes can influence the MFT of the rock. The size effect on the fracture toughness and the reasons for the variation of the MFT were also discussed.

The MFT determined by this testing method will be helpful to interpret the fracture behavior of rocks more accurately. By considering the MFT, the effect of the microstructures of rocks on the fracture behavior can be explained quantitatively. However, more experiments will be necessary to verify its repeatability, and, as

future work, we will perform additional MFT tests for artificial crystals of quartz in consideration of the existence of crystallographic axes, other types of mineral grains, and grain boundaries within rocks. The validation of the MFT estimated in this study might also require the use of other approaches, such as the J integral method and theoretical estimates of ideal K_{IC} of minerals (Tromans and Meech 2002,2004). Furthermore, if the MFT is used as a parameter of the numerical simulation for rock fracturing, this will lead to further understanding of the fracture mechanisms of rock.

References

Amethyst Galleries, Inc., 1995, "The Mineral Quartz," Amethyst Galleries' Mineral Gallery, https://web.archive.org/web/20170601021309/http://www.galleries.com/quartz (accessed 1 June 2017).

Association for Geological Collaboration in Japan, 1996, *Cyclopedia of Earth Science* (in Japanese), Heibonsha Ltd., Tokyo, Japan, 1840p.

Ayatollahi, M. R. and Akbardoost, J., 2014, "Size and Geometry Effects on Rock Fracture Toughness: Mode I Fracture," *Rock Mech. Rock Eng.*, Vol. 47, No. 2, pp. 677–687, https://doi.org/10.1007/s00603-013-0430-7

Bahat, D., Rabinovich, A., and Frid, V., 2001, "Fracture Characterization of Chalk in Uniaxial and Triaxial Tests by Rock Mechanics, Fractographic and Electromagnetic Radiation Methods," *J. Struct. Geol.*, Vol. 23, No. 10, pp. 1531–1547, https://doi.org/10.1016/S0191-8141(01)00018-9

Barker, L. M., 1979, "Theory for Determining K_{Ic} from Small, Non-LERM Specimens, Supported by Experiments on Aluminum," *Int. J. Fract.*, Vol. 15, No. 6, pp. 515–536, https://doi.org/10.1007/BF00019921

Bažant, Z. P., 1984, "Size Effect in Blunt Fracture: Concrete, Rock, Metal," *J. Eng. Mech.*, Vol. 110, No. 4, pp. 518–535, https://doi.org/10.1061/(ASCE)0733-9399(1984)110:4(518)

Bažant, Z. P., Gettu, R., and Kazemi, M. T., 1991, "Identification of Nonlinear Fracture Properties from Size Effect Tests and Structural Analysis Based on Geometry-Dependent R-Curves," *Int. J. Rock Mech. Min. Sci. Geomech. Abstr.*, Vol. 28, No. 1, pp. 43–51, https://doi.org/10.1016/0148-9062(91)93232-U

Cho, S. H., Ogata, Y., and Kaneko, K., 2003, "Strain-Rate Dependency of the Dynamic Tensile Strength of Rock," *Int. J. Rock Mech. Min. Sci.*, Vol. 40, No. 5, pp. 763–777, https://doi.org/10.1016/S1365-1609(03)00072-8

Fowell, R. J., 1995, "Suggested Method for Determining Mode I Fracture Toughness Using Cracked Chevron Notched Brazilian Disc (CCNBD) Specimen," *Int. J. Rock Mech. Min. Sci. Geomech. Abstr.*, Vol. 32, No. 1, pp. 57–64, https://doi.org/10.1016/0148-9062(94)00015-U

Franklin, J. A., Zongqi, S., Atkinson, B. K., Meredith, P. C., Rummel, F., Mueller, W., Nishimatsu, Y., Takahahsi, H., Costin, L. S., Ingraffea, A. R., and Bobrov, G. F., 1988, "Suggested Methods for Determining the Fracture Toughness of Rock," *Int. J. Rock Mech. Min. Sci. Geomech. Abstr.*, Vol. 25, No. 2, pp. 71–96.

Gopalakrishnan, K. and Mecholsky, J. J., Jr., 2012, "Quantitative Fractography of Mixed-Mode Fracture in Soda Lime Silica Glass," *J. Am. Ceram. Soc.*, Vol. 95, No. 11, pp. 3622–3627, https://doi.org/10.1111/j.1551-2916.2012.05431.x

Halford, T. P., Takashima, K., Higo, Y., and Bowen, P., 2005, "Fracture Tests of Microsized TiAl Specimens," *Fatigue Fract. Eng. Mater. Struct.*, Vol. 28, No. 8, pp. 695–701, https://doi.org/10.1111/j.1460-2695.2005.00893.x

Higo, Y., Takashima, K., Shimojo, M., Sugiura, S., Pfister, B., and Swain, M. V., 2000, "Fatigue Testing Machine of Micro-Sized Specimens for MEMS Applications," presented at the *MRS Symposium*, Boston, MA, Materials Research Society, Warrendale, PA, pp. 241–246.

Jeong, S. S., Nakamura, K., Yoshioka, S., Obara, Y., and Kataoka, M., 2017, "Fracture Toughness of Granite Measured Using Micro to Macro Scale Specimens," presented at the *ISRM European Rock Mechanics Symposium (EUROCK 2017)*, Ostrava, the Czech Republic, International Society for Rock Mechanics, Lisbon, Portugal, pp. 761–767.

Jeong, S. S., Obara, Y., and Kataoka, M., 2016, "Evaluation of Microscopic Fracture Toughness of Grains within Granite Using a New Mechanical Testing Machine for Micro-Sized Specimen," presented at the *ISRM European Rock Mechanics Symposium (EUROCK 2016)*, Cappadocia, Turkey, International Society for Rock Mechanics, Lisbon, Portugal, pp. 205–210.

Kataoka, M., Ito, T., Takashima, K., and Obara, Y., 2014, "A New Testing Method to Estimate Microscopic Fracture Toughness of Rock," presented at the *Eleventh ISRM Regional Rock Mechanics Symposium (ROCKMEC'2014)*, Afyonkarahisar, Turkey, International Society for Rock Mechanics, Lisbon, Portugal, pp. 91–96.

Kataoka, M. and Obara, Y., 2013, "Estimation of Fracture Toughness of Different Kinds of Rocks under Water Vapor Pressure by SCB Test (in Japanese)," *J. MMIJ*, Vol. 129, No. 7, pp. 425–432, https://doi.org/10.2473/journalofmmij.129.425

Kataoka, M. and Obara, Y., 2015, "Size Effect in Fracture Toughness of Sandstone," presented at the *13th ISRM International Congress of Rock Mechanics*, Montreal, Canada, International Society for Rock Mechanics, Lisbon, Portugal.

Kataoka, M., Obara, Y., and Kuruppu, M., 2011, "Estimation of Fracture Toughness of Anisotropic Rocks by SCB Test and Visualization of Fracture by Means of X-ray CT," presented at the *Twelfth ISRM International Congress*, Beijing, China, International Society for Rock Mechanics, Lisbon, Portugal, pp. 667–670.

Kataoka, M., Obara, Y., and Kuruppu, M., 2015, "Estimation of Fracture Toughness of Anisotropic Rocks by Semi-circular Bend (SCB) Tests under Water Vapor Pressure," *Rock Mech. Rock Eng.*, Vol. 48, No. 4, pp. 1353–1367, https://doi.org/10.1007/s00603-014-0665-y

Kuruppu, M. D., Obara, Y., Ayatollahi, M. R., Chong, K. P., and Funatsu, T., 2014, "ISRM-Suggested Method for Determining the Mode I Static Fracture Toughness Using Semi-circular Bend Specimen," *Rock Mech. Rock Eng.*, Vol. 47, No. 1, pp. 267–274, https://doi.org/10.1007/s00603-013-0422-7

Liu, H. Y., Kou, S. Q., Lindqvist, P.-A., and Tang, C. A., 2002, "Numerical Simulation of the Rock Fragmentation Process Induced by Indenters," *Int. J. Rock Mech. Min. Sci.*, Vol. 39, No. 4, pp. 491–505, https://doi.org/10.1016/S1365-1609(02)00043-6

Lutgens, F. K. and Tarbuck, E. J., 1997, *Essentials of Geology*, 6th ed., Prentice Hall, Upper Saddle River, NJ, 450p.

Matsuki, K., Hasibuan, S. S., and Takahashi, H., 1991, "Specimen Size Requirements for Determining the Inherent Fracture Toughness of Rocks According to the ISRM Suggested Methods," *Int. J. Rock Mech. Min. Sci. Geomech. Abstr.*, Vol. 28, No. 5, pp. 365–374, https://doi.org/10.1016/0148-9062(91)90075-W

Murakami, Y., 1987, *Stress Intensity Factors Handbook, Vol. 1*, Pergamon Press, Oxford, United Kingdom, 1566p.

Nasseri, M. H. B. and Mohanty, B., 2008, "Fracture Toughness Anisotropy in Granitic Rocks," *Int. J. Rock Mech. Min. Sci.*, Vol. 45, No. 2, pp. 167–193, https://doi.org/10.1016/j.ijrmms.2007.04.005

Nave, C. R., 2017, "Feldspar," *HyperPhysics*, https://web.archive.org/web/20170601021803/https://hyperphysics.phy-astr.gsu.edu/hbase/Geophys/feldspar.html (accessed 1 June 2017).

Shin, K., Okubo, S., Fukui, K., and Hashiba, K., 2005, "Variation in Strength and Creep Life of Six Japanese Rocks," *Int. J. Rock. Mech. Min. Sci.*, Vol. 42, No. 2, pp. 251–260, https://doi.org/10.1016/j.ijrmms.2004.08.009

Takashima, K. and Higo, Y., 2005, "Fatigue and Fracture of a Ni-P Amorphous Alloy Thin Film on the Micrometer Scale," *Fatigue Fract. Eng. Mater. Struct.*, Vol. 28, No. 8, pp. 703–710, https://doi.org/10.1111/j.1460-2695.2005.00923.x

Tang, C., 1997, "Numerical Simulation of Progressive Rock Failure and Associated Seismicity," *Int. J. Rock Mech. Min.*

Sci., Vol. 34, No. 2, pp. 249–261, https://doi.org/10.1016/S0148-9062(96)00039-3

Tromans, D. and Meech, J. A., 2002, "Fracture Toughness and Surface Energies of Minerals: Theoretical Estimates for Oxides, Sulphides, Silicates and Halides," *Miner. Eng.*, Vol. 15, No. 12, pp. 1027–1041, https://doi.org/10.1016/S0892-6875(02)00213-3

Tromans, D. and Meech, J. A., 2004, "Fracture Toughness and Surface Energies of Covalent Minerals: Theoretical Estimates," *Miner. Eng.*, Vol. 17, No. 1, pp. 1–15, https://doi.org/10.1016/j.mineng.2003.09.006

Weibull, W., 1951, "A Statistical Distribution Function of Wide Applicability," *J. Appl. Mech.*, Vol. 18, pp. 293–297.